Vol. 706: 73–89, 2023
https://doi.org/10.3354/meps14233

MARINE ECOLOGY PROGRESS SERIES
Mar Ecol Prog Ser

Published February 23

Differential clearance rates of microbial phylotypes by four appendicularian species

Ayelet Dadon-Pilosof[1,2,*], Keats Conley[3], Fabien Lombard[4,5], Kelly R. Sutherland[3], Amatzia Genin[2,6], Michael Richter[7], Frank Oliver Glöckner[8,9], Gitai Yahel[1]

[1]Faculty of Marine Sciences, Ruppin Academic Center, Mikhmoret 4029700, Israel
[2]Department of Ecology, Evolution & Behavior, The Hebrew University of Jerusalem, Jerusalem 9190401, Israel
[3]Oregon Institute of Marine Biology, University of Oregon, OR 97420, USA
[4]Sorbonne Université, Institut de la Mer de Villefranche-sur-Mer (IMEV), Laboratoire d'Océanographie de Villefranche-sur-Mer, 06230 Villefranche-sur-Mer, France
[5]Institut Universitaire de France, 75005 Paris, France
[6]The Interuniversity Institute for Marine Sciences of Eilat, Eilat 88103, Israel
[7]Ribocon GmbH, Fahrenheitstr. 1, 28359 Bremen, Germany
[8]Alfred Wegener Institute, Helmholtz Center for Polar and Marine Research, Am Handelshafen 12, 27570 Bremerhaven, Germany
[9]Jacobs University, Campus Ring 1, Bremen gGmbH, 28759 Bremen, Germany

ABSTRACT: Appendicularians are abundant planktonic filter feeders that play a significant role in the pelagic food web due to their high clearance rates. Their diet and feeding rates have typically been measured as bulk chlorophyll or cell removal, with some attention given to prey size but no differentiation between the microbial phylotypes. Using a combination of *in situ* and laboratory incubations with flow cytometry and next-generation sequencing, we found species-specific differences in clearance rates and diet compositions of 4 common species: *Oikopleura albicans*, *O. fusiformis*, *O. longicauda*, and *O. dioica*. While *O. albicans* most efficiently removed nano-eukaryotic algae, the other smaller species preferentially removed micron-sized pico-eukaryotic algae. Pico- and nano-eukaryotic cells constituted the major food source of the studied appendicularians despite their occurrence in oligotrophic water dominated by prokaryotic cells. Across species, pico- and nano-planktonic microalgae biomass comprised 45 to 75% of the appendicularian diets. Although non-photosynthetic bacteria were removed at lower rates than all other prey groups, their total contribution to the appendicularian diet was not trivial, representing 5 to 19% of the planktonic carbon in the appendicularian diet; pico-cyanobacteria contributed an additional 9 to 18%. Removal rates and efficiencies of pico-eukaryotes were higher than those of prokaryotes of similar size. Strikingly different clearance rates were observed for different prokaryotic phylotypes, indicating that factors other than size are involved in determining the capturability of the cells. Collectively, our findings provide additional evidence for differential retention of microbial prey among mucous-mesh grazers and its substantial effect on the upper-ocean microbial community.

KEY WORDS: Pelagic food webs · Clearance rate · Differential retention · Tunicates · SAR11 · Suspension feeders

*Corresponding author: ayelet@ruppin.ac.il

1. INTRODUCTION

Appendicularians are globally distributed gelatinous grazers, often the second or third most abundant zooplankton taxa in the euphotic zone (Alldredge 1976a). At times, their abundance can rival that of copepods, while their higher feeding and growth rates (Lombard et al. 2010a) make their secondary production rate 35 to 71% higher than that of copepods (Hopcroft & Roff 1998). Appendicularians are considered microphagous grazers that can capture pico- and small nano-plankton with unusually high efficiency compared to other similarly sized mesozooplankton (Sommer et al. 2002, Tönnesson et al. 2005).

The appendicularian prey-to-predator size ratio spans 3 orders of magnitude, from ~10^{-3} to 10^{-1} (Lombard et al. 2011). An external mucous filter house enables them to collect and ingest a wide spectrum of prey sizes, including viruses (Lawrence et al. 2018), colloids (Flood et al. 1992), bacteria (King et al. 1980, Bedo et al. 1993, Fernández et al. 2004, Tönnesson et al. 2005), nano-plankton (Gorsky et al. 1999, Tönnesson et al. 2005), and ciliates (Lombard et al. 2010b). The sinusoidal beating of the animal's tail drives and controls flow through the house (Selander & Tiselius 2003), achieving high filtration rates ranging from ~100 to ~1000 ml individual^{-1} d^{-1} (Alldredge 1981).

The size, morphology, and chemical composition of the house is family- and species-specific (Alldredge 1976a,b). Houses vary in solidity, from mucilaginous to gelatinous, and also in their carbon and nitrogen compositions (Alldredge 1976b). The houses of most species have inlet filters to exclude large or spinous particles from entering them, but a few species, such as *Oikopleura longicauda* and *Mesochordaeus erythrocephalus*, lack these pre-filters (Alldredge 1977, Hopcroft & Robison 1999). Within the house, the food-concentrating filter traps particles, which are conveyed to the pharyngeal filter, the third and final filter that captures particles for ingestion (Conley et al. 2018a).

Inherently, this filtration process depends, in part, on particle size. The inlet filters, when present, act as a coarse sieve to exclude particles at the upper size range (Alldredge 1977). This is determined by the pore size, pore shape, and variance in relation to the prey particles (Silvester 1983, Lombard et al. 2010b). The food-concentrating filter acts as a tangential flow filter on which smaller particles are more likely to remain stuck (Conley et al. 2018a). The pharyngeal filter has a coarser pore size than the food-concentrating filter (Deibel & Powell 1987), so effective capture relies heavily on coagulating small particles into aggregates larger than the pharyngeal filter pores (Deibel & Lee 1992, Tiselius et al. 2003). In addition, because appendicularian filtration occurs at low Reynolds numbers, particles smaller than the mesh pores can be retained via diffusional deposition and direct interception (Rubenstein & Koehl 1977, Acuña et al. 1996). Since the filtration process does not follow a simple sieve model, other factors, such as surface properties, can affect retention efficiency (Gerritsen & Porter 1982, Conley et al. 2018b and references therein).

Mesh morphology, animal behavior, hydrodynamics, and particle properties can play important roles in determining particle selection by mucous-mesh grazers (reviewed in Conley et al. 2018b). Recent methodological developments have expanded our ability to understand the selectivity of pelagic tunicates (reviewed in Sutherland & Thompson 2022). In particular, flow cytometry techniques and next-generation sequencing have greatly advanced our ability to quantify feeding on microbial populations. These tools can provide more information on grazer selectivity, with high resolution of size and taxonomy (Sutherland & Thompson 2022).

Prior investigations, which pre-dated these newer tools, largely considered appendicularian feeding as non-selective (Bedo et al. 1993, Dagg et al. 1996, Gorsky et al. 1999, Tönnesson et al. 2005). However, several behavioral and physical mechanisms allow appendicularians to reject particles (Lombard et al. 2011, Conley et al. 2018b). Furthermore, as initially demonstrated by Gerritsen & Porter (1982) and recently re-affirmed by Dadon-Pilosof et al. (2017) and Jacobi et al. (2021), surface property interactions between prey cells and the filter result in size-independent retention efficiencies. Taken together, the complex morphology, surface properties, behavior, and hydrodynamics of particle capture by appendicularians can manifest as apparent 'preference' or 'selectivity' toward specific prey populations.

In this study, we examined appendicularian filtration on a natural assemblage of pico- and nano-plankton and tested the null hypothesis that removal of the different prey types is non-selective. To do so, we used a combination of *in situ* and laboratory incubation experiments with 4 oikopleurid species exposed to 2 distinct oligotrophic planktonic prey assemblages from the Northwest Mediterranean Sea (NWMS) and the North Sea.

2. MATERIALS AND METHODS

Our study was carried out near the bay of Villefranche-sur-Mer, France, in the NWMS (43° 42' N, 7° 18' E), where the bottom depth is >100 m. The underwater work was carried out at 8 to 15 m depth by SCUBA divers during the spring (23 to 30 April 2014), coinciding with an appendicularian bloom in which divers could encounter several individuals per minute. A set of *in situ* experiments (see Section 2.1) was complemented with laboratory incubations using freshly collected seawater from the field site.

2.1. *In situ* incubations

To study appendicularians feeding in their natural habitat and to minimize disturbance to these small (<3 mm), fragile planktonic tunicates, we modified the indirect clearance rate (CR) method techniques described by Riisgård (2001). Using blue-water SCUBA, we identified specimens from 3 species (*Oikopleura albicans*, *O. fusiformis*, and *O. longicauda*) during drift dives in the open sea. The incubation cylinders (10 cm long, 2.5 cm diameter) were built by gluing together 2 Falcon tubes (20 ml) from which the lower conical section was removed. Underwater, the open-ended cylinder (~20 ml) was carefully positioned over each individual and both sides were gently closed. Care was taken to avoid any contact between the animal and the tube walls. A control sample with no animal inside was immediately collected using an identical cylinder. The closed cylinders were suspended at the depth of collection (8 to 15 m) for ~0.5 to 1.5 h by attaching them to a free-drifting frame suspended by a line to 2 surface floats. At the end of the incubation, the cylinders were gently transferred to an ice-filled cooler on a boat, where a 7 ml water sample was carefully withdrawn from each cylinder. The sample was withdrawn using a pipette attached to a tube that was gently inserted into the cylinder without touching the animal inside. The opening of the tube was covered with a piece of mesh (120 µm pore size) to exclude larger organisms from the sampled water. The samples were stored on ice in a dark cooler until laboratory processing within 4 h.

Because accurate species-level identifications were difficult underwater, at the end of the incubation, each incubator was drained into a Petri dish and inspected under a dissecting microscope for the presence of animals and houses. Each individual was photographed for subsequent length measurements, and species were identified when possible. Body lengths were measured in image analysis (Image J) following Lombard et al. (2010a) (see summary in Table 1). Using a wire probe, houses were carefully transferred into a microtube and kept frozen at −80°C.

2.2. Particle composition of discarded houses

Analysis of microbial communities in the discarded appendicularian houses was performed to elucidate the type of particles that adhere to house filters. Following the completion of the *in situ* incubation experiments, we collected 12 discarded houses from *O. albicans* and 3 from each of *O. fusiformis* and *O. longicauda*. From each house, DNA was extracted and sequenced for 16S rRNA (see Sections 2.4.2 to 2.4.4), and the relative abundance of each phylotype was compared to its relative abundance in the corresponding ambient water samples taken at the start (T_0) and end of the incubation (T_f).

2.3. Laboratory incubations

Since *O. dioica*, a common species in the NWMS and other seas, was not encountered during our fieldwork, we studied the feeding of this species using laboratory incubations and cultured specimens (see Section 2.3.1). Laboratory incubations with *O. dioica* were performed both during our study in Villefranche-sur-Mer (April 2014) and at the Sars International Centre for Marine Molecular in Bergen, Norway (December 2015), as described in Section 2.3.2. It should be noted that the plankton composition in these 2 localities was very different; hence, the phylogenetic composition of the different planktonic categories (e.g. 'nano-plankton' or 'HNA-Hs' [high nucleic acid, high-scatter non-photosynthetic bacteria]) was also very different between these 2 experiments.

2.3.1. NWMS

The *O. dioica* stock for this experiment were originally from the Sars International Centre (Espegrend Marine Field Station Espelandsvegen, Norway; www.uib.no/en/bio/53898/marine-biological-station-espegrend), and were grown for 3 generations at the laboratory in Villefranche. The individuals for this experiment were from the third

generation of cultures reared at Villefranche and were all 5 d old individuals. Surface seawater for the experiment was collected outside the bay of Villefranche-sur-Mer (~14°C) and was pre-filtered through a 120 µm nylon mesh into 30 ml polystyrene tubes. Five individuals were carefully transferred from the 10 l culture beakers into each experimental tube (30 ml) with pre-filtered seawater. Incubations were performed under low illumination in a temperature-controlled room (15.5°C). After a 1 h incubation, water was carefully sampled from each incubator as described above for the field incubations. Three control incubators without animals were also sampled at T_0 and T_f.

2.3.2. North Sea

Cultured *O. dioica* (5 d old) grown at the appendicularian culture facility at the Sars International Centre for Marine Molecular Biology were used for this experiment. Surface water (10 m depth, 9°C) was collected at the Espegrend Marine Field Station Espelandsvegen, Norway (60° 16′ N, 5° 13′ E). At the Sars Centre, the seawater temperature was slowly raised to 14.5°C using a water bath to match culture conditions, then pre-filtered through a 21 µm mesh. The experimental design was slightly modified from that of the Mediterranean spring incubation and included larger incubators to mimic culture conditions, thereby minimizing changes to animal behavior. A total of 10 individuals were incubated in each of 10 glass Pyrex (1 l) beakers containing 1 l of the pre-filtered seawater (21 µm). Each beaker was equipped with a slowly rotating paddlewheel that mixed the water and kept the animals in suspension. The incubation was conducted under low illumination on a lab bench (16.2°C at T_0, 17.7°C at T_f). Water samples (~1.5 ml) were collected at T_0, and then at 1 and 2 h after the initiation of the experiment. Five identical control incubators without animals were sampled at T_0 and at each time point during the incubation. Sample analysis indicated that the animals' filtration during the first hour of incubation was much reduced (e.g. see Fig. 3 vs. Fig. S2 in the Supplement at www.int-res.com/articles/suppl/m706p073_supp.pdf), likely reflecting an acclimation period to the new water and/or building of new houses after transfer. Therefore, we consider the samples taken 1 h after initiation of the incubation as T_0 for this experiment and samples taken 2 h after incubation as T_f.

2.4. Sample analysis

2.4.1. Flow cytometry

Flow cytometry was used to quantify the concentrations and cell characteristics of non-photosynthetic microbes (hereafter referred to as non-photosynthetic bacteria) and the 4 dominant autotrophic groups: *Prochlorococcus* (Pro), *Synechococcus* (Syn), pico-eukaryotic algae (PicoEuk), and nano-eukaryotic algae (NanoEuk). We used an Attune® Acoustic Focusing Flow Cytometer (Applied Biosystems) equipped with a syringe-based fluidic system that allows precise adjustment of the injected sample volume and hence high precision of the measurements of cell concentrations (±5%). The optics system contained violet and blue lasers (405 and 488 nm, respectively) and was further adapted for the analysis of marine ultra-plankton samples.

Aliquots of 1.8 ml were collected from each water sample and transferred into 2 ml cryovials (Corning cat. no. 430659). Samples were first incubated for 15 min at room temperature with Glutaraldehyde 50% (electron microscopy grade; Sigma-Aldrich, cat. no. 340855) at 0.2% (final concentration) for the more productive NWMS water. Samples were frozen in liquid nitrogen (at least 60 min) and then stored at −80°C until analysis (within a few weeks).

Each sample was analyzed twice. First, 600 µl of the sample water was analyzed at a high flow rate (100 µl min^{-1}) for the determination of ultra-phytoplankton with a dual threshold (trigger) on the red fluorescence channels of the violet and blue lasers. A second run was used to analyze cells with no autofluorescence, i.e. non-photosynthetic bacteria. To visualize these cells, a 300 µl aliquot of the sample water was incubated with the nucleic acid stain SYBR Green I (20 to 120 min dark incubation at room temperature; $1:10^4$ of SYBR Green commercial stock). For this run, we used a low flow rate of 25 µl min^{-1}, and the instrument was set to high-sensitivity mode. A 755 µl aliquot of the sample water was analyzed with a dual threshold (trigger) on green fluorescence channels of the violet and blue lasers.

Taxonomic discrimination was made based on orange fluorescence (Bl2, 574 ± 13 nm) of phycoerythrin and red fluorescence (Bl3, 690 ± 20 nm and VL3, 685 ± 20 nm) of chlorophyll (Tarao et al. 2009). Side scatter (SSC) provides a proxy of cell surface complexity and cell volume (Marie et al. 1999), whereas forward scatter (FSC) is considered the best proxy of cell size (Cunningham & Buonnacorsi 1992, Simon et al. 1994). As a rough proxy of the cell size of

each planktonic cell population, we used the ratio of the median FSC of the respective cell population to the median FSC of reference beads (Polysciences™, cat. no. 23517; Flow Check High-Intensity Green Alignment 1.0 µm) that were used as an internal standard in each sample. While this ratio provides a relatively robust estimate of cell size for cells larger than 1 µm, it very likely underestimates the sizes of submicron particles. See Dadon-Pilosof et al. (2019) for a further discussion of the accuracy of size estimates.

Where possible, the non-photosynthetic bacteria were further divided based on their green fluorescence (a proxy for nucleic acid content) and FSC (the proxy for size) into 3 groups: low nucleic acid, non-photosynthetic bacteria (LNA); high nucleic acid, low-scatter non-photosynthetic bacteria (HNA-Ls); and high nucleic acid, high-scatter non-photosynthetic bacteria (HNA-Hs) (Zubkov et al. 2004). Similarly, the eukaryotic algae were separated into PicoEuk and NanoEuk (Simon et al. 1994). For PicoEuk, we followed Worden & Not (2008), which suggested a size range of up to 3.0 µm, while larger eukaryotes were designated as NanoEuk (3.0 to 20 µm). The literature regarding Syn size is vague but the reported size range is 0.3 to 1.2 µm (e.g. Uysal 2001, Garcia et al. 2016). A cluster of Pro-like particles (PLPs) with low FSC (very small size), significant red fluorescence, and low or null orange fluorescence was present in all water types and seasons. The ratio of the median FSC of this cell population to the median FSC of 1 µm yellow-green reference beads that were run with each sample ranged from 0.01 to 0.3. This ratio is considerably lower than the best estimates for Pro cell size that were made on cultures and provided a range of 0.5 to 0.8 µm for length and 0.4 to 0.6 µm for width (Partensky et al. 1999). Therefore, while this low ratio is most likely a consequence of a low refractive index of these cells, we conservatively refer to these very small particles as PLPs.

2.4.2. DNA extraction

The relative abundance of the different prokaryotic taxa (phylotypes) in the seawater, before and after being filtered by the appendicularians and/or adhering to their houses, was quantified using next-generation sequencing of the 16S V1–V3 region in order to detect any differential filtration of different phylotypes. Due to the limited volume of water available, we applied the small volume extraction method developed by Dadon-Pilosof et al. (2017). Briefly, a small amount of seawater (5 to 10 ml) was collected from each incubator and filtered on a 25 mm, 0.2 µm polycarbonate membrane (GE Healthcare Biosciences, cat. no. 110606) under low vacuum and frozen in 1.5 ml micro-tubes at −20°C until analysis.

DNA from each filter was extracted using the DNeasy 'Blood & tissue kit' (Qiagen, cat. no. 69504), with the following modifications to the manufacturer's protocol: ATL buffer (180 µl) and 20 µl of Proteinase K were added and samples were incubated at 56°C for 1 h. Then, 200 µl of AL buffer and 200 µl of 95 to 100% ethanol were added to the sample and the mixture was pipetted into spin columns and placed in a 2 ml collection tube. Tubes were centrifuged at 6000 relative centrifugal force (RCF) for 1 min. The flow-through was discarded and 500 µl of AW1 buffer was added to the column, centrifuged at 6000 RCF for 1 min, and the flow-through again discarded. This step was repeated for a third time, with 500 µl buffer AW2 and a spin of 18 000 RCF for 1 min to dry the membrane before elution. For the elution step, the spin column was placed on a new collection tube. Then, 200 µl of buffer AE, preheated to 56°C, was pipetted at 3 steps (50, 50, and 100 µl) into the column; each step was followed by 6000 RCF centrifugation for 1 min. The sample was then incubated at room temperature for at least 1 min and stored at −20°C.

2.4.3. Next-generation sequencing

Samples were amplified for sequencing using a forward and reverse fusion primer (28F-519R, 16S V1–V3 region). The forward primer was constructed with (5′–3′) the Illumina i5 adapter (AAT GAT ACG GCG ACC ACC GAG ATC TAC AC), an 8 to 10 bp barcode, a primer pad, and the 5′-GAG TTT GAT CNT GGC TCA G-3′ primer. The reverse fusion primer was constructed with (5′–3′) the Illumina i7 adapter (CAA GCA GAA GAC GGC ATA CGA GAT), an 8 to 10 bp barcode, a primer pad, and the 5′-GTN TTA CNG CGG CKG CTG-3′ primer. Primer pads were designed to ensure the primer pad/primer combination had a melting temperature of 63 to 66°C, according to methods developed by the lab of Patrick Schloss (www.mothur.org/w/images/0/0c/Wet-lab_MiSeq_SOP.pdf). Amplifications were performed in 25 µl reactions with Qiagen HotStar Taq master mix (Qiagen), 1 µl of each 5 µM primers, and 1 µl of the template. Reactions were performed on ABI Veriti thermocyclers (Applied Biosystems) under the following thermal profile: 95°C for 5 min, then 35

cycles of 94°C for 30 s, 54°C for 40 s, 72°C for 1 min, followed by 1 cycle of 72°C for 10 min and 4°C hold.

Amplification products were visualized with eGels (Life Technologies). Products were then pooled equimolar, and each pool was size-selected in 2 rounds using Agencourt AMPure XP (Beckman-Coulter) in a 0.7 ratio for both rounds. Size-selected pools were then quantified using the Qubit 2.0 fluorometer (Life Technologies) and loaded on an Illumina MiSeq (Illumina) 2 × 300 flow cell at 10 pM.

2.4.4. Bioinformatics

All sequence reads were processed by the next-generation sequencing analysis pipeline of the SILVA rRNA gene database project (SILVAngs 1.3; Robertson & Button 1989). Each read was aligned using the SILVA Incremental Aligner (SINA v.1.2.10 for ARB SVN, revision 21008) (Robertson & Button 1989) against the SILVA SSU rRNA SEED and quality controlled (Pruesse et al. 2012). Reads shorter than 50 aligned nucleotides and reads with more than 2% of ambiguities, or 2% of homopolymers, respectively, were excluded from further processing. Putative contamination and artefact reads with a low alignment quality (50 alignment identity, 40 alignment score reported by SINA) were identified and excluded from downstream analysis. After these initial steps of quality control, identical reads were identified (dereplication), the unique reads were clustered into operational taxonomic units (OTUs) on a per-sample basis, and the reference read of each OTU was classified. Dereplication and clustering were done using cd-hit-est v.3.1.2 (www.bioinformatics.org/cd-hit) (Quast et al. 2013) running in accurate mode, ignoring overhangs, and applying identity criteria of 1.00 and 0.98, respectively. The classification was performed by a local nucleotide BLAST search against the non-redundant version of the SILVA SSU Ref data set (release 123; www.arb-silva.de) using BLASTn v.2.2.30+ (http://blast.ncbi.nlm.nih.gov/Blast.cgi) with standard settings (Li & Godzik 2006).

The classification of each OTU reference read was mapped onto all reads that were assigned to the respective OTU. This yields quantitative information (number of individual reads per taxonomic path) within the limitations of PCR and sequencing technique biases as well as multiple rRNA operons. Reads without any BLAST hits or reads with weak BLAST hits, where the function '% sequence identity + % alignment coverage)/2' did not exceed the value of 93, remained unclassified. These reads were assigned to the meta-group 'No Relative' in the SILVAngs fingerprint and Krona charts (Camacho et al. 2009).

The SAR11 OTUs were renamed using the widely recognized clades initially described by Suzuki et al. (2001) (clades I and II), later expanded by Morris et al. (2005) (clades II and IV), and subsequently used by recognized authors in the SAR11 field (e.g. Carlson et al. 2009, Brown et al. 2012, Vergin et al. 2013). The OTUs were reassigned by inserting representative sequences from each SILVA SAR11 clade into a SAR11 phylogenetic tree constructed in the ARB program using full-length sequences that defined clades I to IV (e.g. Vergin et al. 2013). The OTUs defined by SILVA as SAR11 S1 and S1* were grouped in the same surface clade I. To avoid a mixture of general and specific labels, the OTU classed as 'SAR11' that did not fall into a defined cluster was classed as SAR11_Unclassified.

2.5. Data analysis

Our experimental setup was designed to test the null hypothesis of non-selective removal of the different prey types. This setup was especially robust due to its pairwise nature (simultaneous incubation vs. control) and the concurrent comparison of the removal of multiple prey taxa that co-occur naturally in the ambient water. Data were therefore analyzed using within-subject comparisons tests, i.e. paired *t*-test and repeated-measures ANOVA (RM-ANOVA), with the CRs of the different prey types as the repeated measures. To circumvent the need to meet RM-ANOVA assumptions of lack of sphericity and compound symmetry, we used Wilks' multivariate test for RM-ANOVA (Davis 2002). Where the assumptions of normality and homogeneity of the variance were not met, we used the nonparametric alternatives: Wilcoxon signed-rank test and Friedman RM-ANOVA on ranks. In cases where the RM-ANOVA showed significant differences between the removal efficiencies of different prey types, the Bonferroni post hoc procedure was used to test for differences between all pairs of prey types.

CR is a common measure of grazing rate in many studies of suspension feeding (e.g. Deibel 1985, Riisgård 2001). It is defined as a virtual volume of water that would have been cleared of all prey cells by an individual grazer per unit of time if the filtration efficiency of these cells was 100%. In cases where the filtration efficiency is indeed 100%, the CR is equal to the pumping or water processing rate (Riisgård

2001 and references therein). In this study, the CR (ml ind.$^{-1}$ h^{-1}) for prey type i was calculated as:

$$CR_i = \frac{V}{n \times t} \times \ln\left(\frac{C_{i,\,con}}{C_{i,\,Inc}}\right) \quad (1)$$

where V is the incubator volume (ml), n is the number of individual appendicularians in the incubator, t is the incubation time (h), and $C_{i,\,Inc}$ and $C_{i,\,con}$ are the concentrations of the i^{th} prey type in the incubator with appendicularians and without appendicularians (control), respectively, by the end of the experiment.

Unlike flow cytometry, which provides exact concentrations of each taxonomic group, Illumina sequencing provides much finer taxonomic resolution (phylotype level) but only a relative frequency of each OTU (phylotype). Therefore, to calculate microbe-specific CRs, we estimated the concentration of each phylotype (C_i) as the product of its relative frequency and the total bacterial cell counts obtained from the flow cytometer.

A measure termed 'relative retention efficiency' ($RE'_{i,j}$) was calculated for each prey type (i) in each sample (j) by normalizing its CR to that of the prey with the highest CR:

$$RE'_{i,j}\,(\%) = 100 \times \frac{CR_{i,j}}{CR_{i,j_{max}}} \quad (2)$$

where CR is the measured clearance rate and j_{max} is the prey population that was retained at the highest rate in that sample (Harbison & McAlister 1979). Note that where the same prey type j was always removed at the highest efficiency, its average RE will be exactly 100%, (e.g. the RE of *O. fusiformis* for PicoEuk was 100%; see Fig. 2), whereas where different taxa are removed at the highest efficiency in different incubations, the average RE will be <100% (e.g. the RE of NanoEuk by *O. albicans*; see Fig. 1).

Hereafter, the use of the terms 'selectivity' and 'preference' are limited to their technical definition (Chesson 1978, 1983), i.e. the removal of a prey type in higher proportion than its proportional presence in the environment relative to other food types present.

The total number of specimens sampled underwater was 47, 21, and 7 for *O. fusiformis*, *O. albicans*, and *O. longicauda*, respectively. In many incubations (25, 5, and 5, respectively), we found no evidence of active cell removal, defined as the removal of >10% of PicoEuk. These cases were excluded from our analysis in order to examine differential prey removal only by actively feeding animals. Appendicularians are quite sensitive to disturbance — for example, Alldredge (1976c, p. 37) described how some species of oikopleurids cease filtering 'when they sensed the divers' presence, thus biasing filtering observations' — but otherwise feed continuously when undisturbed (Alldredge 1976c, 1981). We therefore conservatively opted to exclude individuals with <10% cell removal under the assumption that this lack of feeding behavior may reflect experimental artefacts. Previous incubation experiments with appendicularians have similarly excluded samples where animals did not exhibit active feeding (Scheinberg et al. 2005). Because of the low sample size for *O. longicauda*, excluding non-feeding individuals rendered only 2 successful replicates for this species. Therefore, the detailed results for this species are reported in the Supplement.

Throughout the text, data are presented as means ± 95% confidence intervals unless stated otherwise.

3. RESULTS

3.1. *In situ* incubations

Cell counts obtained with a flow cytometer indicated that *Oikopleura albicans* exhibited size-dependent filtration, with preferential removal and high CRs of prey larger than 1 µm (24 ± 11 and 14 ± 6.5 ml ind.$^{-1}$ h^{-1} for NanoEuk and PicoEuk, respectively; RM-ANOVA, Wilks' λ = 0.27, $F_{6,8}$ = 3.7, p = 0.046; Fig. 1a,b, Table 1). The more abundant small pico-cyanobacteria (PLPs and Syn) ($3.7 \times 10^4 \pm 1.8 \times 10^4$ cells ml^{-1}) and bacteria with high nucleic acid content (i.e. HNA-Hs) ($7.8 \times 10^4 \pm 4.1 \times 10^4$ cells ml^{-1}) were removed at a reduced CR (8.5 ± 4.2 and 8.7 ± 7.3 ml ind.$^{-1}$ h^{-1} for pico-cyanobacteria and HNA-Hs, respectively; Fig. 1a,b). No significant removal was observed for the LNA (2.1 ± 2.9 ml ind.$^{-1}$ h^{-1}; Fig. 1c) that are usually associated with the SAR11 clade (Mary et al. 2006). Surprisingly, within the NanoEuk, smaller algae were removed more efficiently than larger nano-eukaryotes, as reflected by a >25% shift of the median FSC of this group in the incubators in comparison to the controls (data not shown). In contrast, within the PicoEuk, the largest cells were preferentially removed.

The ambient concentration of microbial cells for the *O. albicans* experiments was $5.4 \times 10^5 \pm 1.1 \times 10^5$ cells ml^{-1} with 20 phylotypes (clustered at 98% identity), accounting for 94% of the total 16S rRNA gene reads sequenced. The SAR11 clade and pico-cyanobacterial phylotypes accounted for 44 and 33% of the total reads, respectively (pink and green shades,

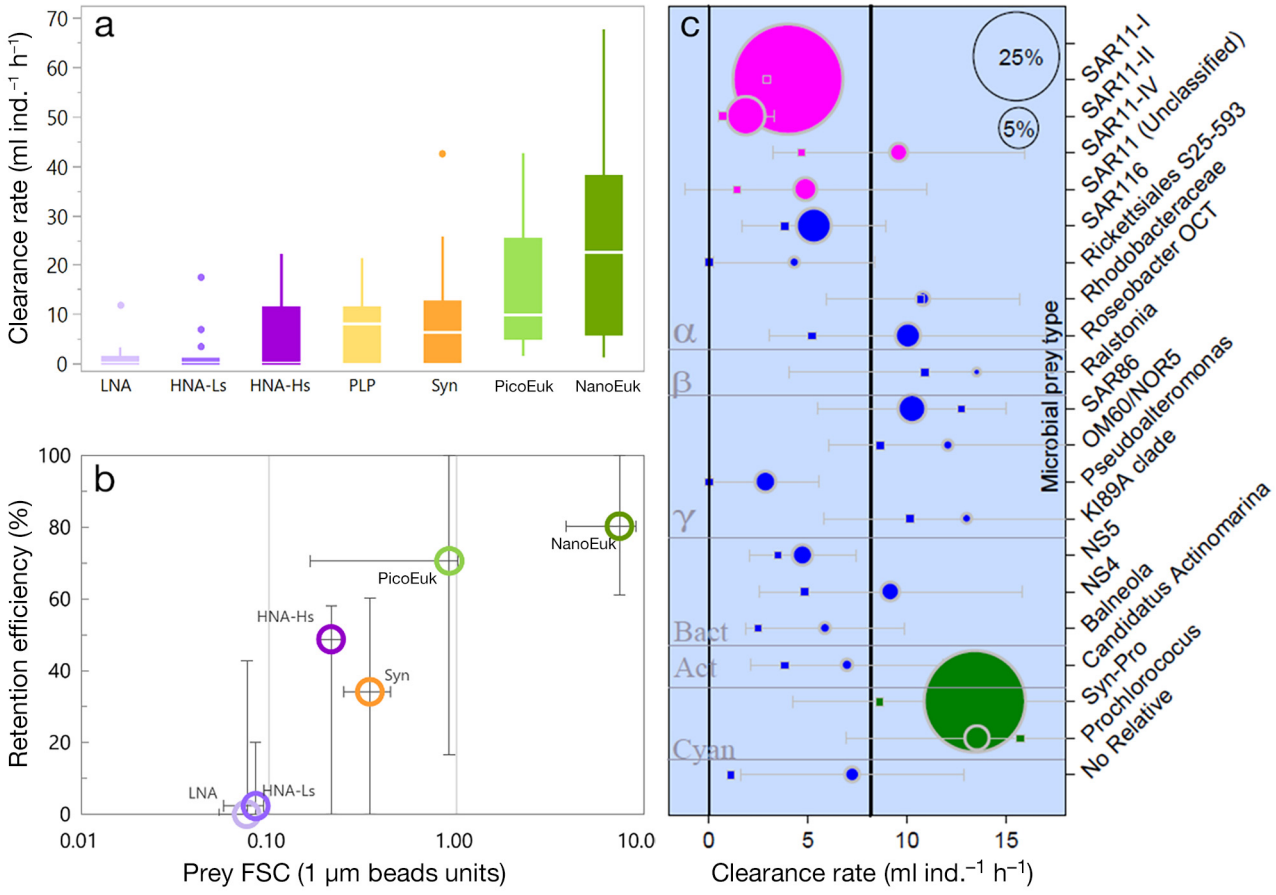

Fig. 1. Differential clearance rates of the appendicularian *Oikopleura albicans* on marine microbes, measured by *in situ* incubations in the Northwest Mediterranean Sea (NWMS) during April 2014 (n = 16). (a) Clearance rates of different prey types were counted with flow cytometry. Eukaryotic cells — NanoEuk: nano-eukaryotic algae and PicoEuk: pico-eukaryotic algae. Pico-cyanobacterial taxa — Syn: *Synechococcus* and PLP: *Prochlorococcus*-like particles. Non-photosynthetic bacteria are subdivided into HNA-Ls: high-nucleic acid low-scatter cells; HNA-Hs: high-nucleic acid high-scatter cells; and LNA: low-nucleic acid cells. Horizontal lines: medians; box limits: 25th and 75th percentiles; whiskers: 1.5× the interquartile range from the 25th and 75th percentiles; dots: outliers. (b) Relation between retention efficiency of different prey types and their relative size, calculated as the ratio of cells' forward scatter (FSC) to the FSC of 1 µm beads, color-coded as in (a). Vertical error bars: lower and upper quartiles of retention efficiency; horizontal error bars: lower and upper quartiles of the FSC normalized to the FSC of 1 µm beads. (c) Clearance rates of the 20 most abundant prokaryotic operational taxonomic units (OTUs) in the water. Grey lines divide OTUs into taxonomic categories. α: *Alphaproteobacteria*; β: *Betaproteobacteria*, γ: *Gammaproteobacteria*; Bact: *Bacteroidetes*; Act: *Actinobacteria*; Cyan: *Cyanobacteria*. Pink: members of the SAR11 clade; green: autotrophs; blue: other non-photosynthetic bacteria. Vertical line: expected clearance rate assuming equal clearance rate probability for all cells (the average over all phylotypes). Circle size represents relative abundance in ambient water during sampling (circles in upper right show the scale for 5 and 25% of total reads). Error bars: 95% CI. Squares: median clearance rates. Reproduced from Dadon-Pilosof et al. (2017) *Nature Microbiology*

respectively, in Fig. 1c). While the water sampled at the end of the incubation had a significantly reduced frequency of pico-cyanobacteria reads (paired *t*-test, $p < 0.001$), the frequencies of reads attributed to the SAR11 OTUs increased, suggesting high removal of pico-cyanobacteria but not SAR11 (Fig. 1c).

In contrast to *O. albicans*, *in situ* incubations showed that *O. fusiformis* preferentially removed PicoEuk (7.4 ± 2.1 ml ind.$^{-1}$ h^{-1}; Fig. 2a,b, Table 1) over both the larger NanoEuk and smaller pico-cyanobacteria (post hoc Bonferroni correction tests, $p < 0.001$; Fig. 2a,b), despite the higher abundance of these latter 2 groups (Table 1). The abundant non-photosynthetic bacteria groups HNA-Ls, HNA-Hs, and LNA, which numerically dominated the planktonic community, were removed by *O. fusiformis* at significantly lower CRs (1.3 ± 0.7, 1.0 ± 1.1, and 0.8 ± 0.5, respectively; post hoc Bonferroni test, $p < 0.05$; Fig. 2a,b). *O. fusiformis* cleared the smaller fraction of both the NanoEuk and PicoEuk more efficiently than larger cells, as reflected by a ~25% shift of the FSC of these groups in the incubators in comparison

Table 1. Appendicularian clearance rates from *in situ* and laboratory experiments. N: number of incubation containers in each experiment. Animal sizes are reported as means ± 95% confidence intervals for the mean and median. **Bold** indicates clearance rates that were significantly different from zero ($p < 0.05$). All abbreviations are as in Fig. 1

Appendicularian species	N	Date and sampling site	Individual size (mm)	Prey type	Ambient concentration (cells ml^{-1}) Mean ± 95% CI	Median ± 95% CI	Clearance rate (ml $ind.^{-1}$ h^{-1}) Mean ± 95%CI	Median
Oikopleura albicans	16	Apr 2014 NWMS (*in situ*)	1.99 ± 0.31 (1.99)	NanoEuk	$2.05 \times 10^3 \pm 4.75 \times 10^2$	1.90×10^3	**24.02 ± 10.89**	**22.58**
				PicoEuk	$1.64 \times 10^3 \pm 5.85 \times 10^2$	1.59×10^3	**14.36 ± 6.53**	**9.82**
				Syn	$5.29 \times 10^4 \pm 2.59 \times 10^3$	5.53×10^4	**9.09 ± 6.28**	**6.17**
				PLP	$2.18 \times 10^4 \pm 6.18 \times 10^4$	2.71×10^4	**7.8 ± 3.68**	**8.00**
				HNA-Ls	$1.27 \times 10^5 \pm 3.77 \times 10^4$	1.38×10^5	3.13 ± 4.51	0.00
				HNA-Hs	$7.97 \times 10^4 \pm 4.18 \times 10^4$	6.74×10^4	**8.74 ± 7.3**	**7.38**
				LNA	$3.28 \times 10^5 \pm 6.56 \times 10^4$	3.24×10^5	2.18 ± 2.9	0.44
O. fusiformis	22	Apr 2014 NWMS (*in situ*)	0.63 ± 0.06 (0.67)	NanoEuk	$2.16 \times 10^3 \pm 3.69 \times 10^2$	1.96×10^3	**2.54 ± 1.06**	**1.89**
				PicoEuk	$2.34 \times 10^3 \pm 5.68 \times 10^2$	2.02×10^3	**7.36 ± 2.08**	**6.44**
				Syn	$4.95 \times 10^4 \pm 4.03 \times 10^3$	4.87×10^4	**1.31 ± 0.87**	**0.19**
				PLP	$2.39 \times 10^4 \pm 3.75 \times 10^3$	2.43×10^4	**3.38 ± 1.21**	**2.66**
				HNA-Ls	$1.59 \times 10^5 \pm 1.64 \times 10^4$	1.61×10^5	**1.33 ± 0.74**	**0.75**
				HNA-Hs	$4.60 \times 10^4 \pm 1.62 \times 10^4$	3.51×10^4	1.01 ± 1.16	0.00
				LNA	$4.15 \times 10^5 \pm 6.17 \times 10^4$	3.92×10^5	**0.8 ± 0.55**	**0.03**
O. longicauda	2	Apr 2014 NWMS (*in situ*)	1.97 ± 0.68 (1.97)	NanoEuk	$1.90 \times 10^3 \pm 5.15 \times 10^3$	1.90×10^3	13.07 ± 106.56	13.07
				PicoEuk	$1.06 \times 10^3 \pm 4.29 \times 10^3$	1.06×10^3	19.18 ± 50.31	19.18
				Syn	$4.92 \times 10^4 \pm 1.69 \times 10^3$	4.92×10^4	7.05 ± 87.4	7.05
				PLP	$1.93 \times 10^4 \pm 1.00 \times 10^5$	1.93×10^4	**13.14 ± 3.92**	**13.14**
				HNA-Ls	$1.32 \times 10^5 \pm 3.17 \times 10^5$	1.32×10^5	3.6 ± 25.58	3.60
				HNA-Hs	$6.33 \times 10^4 \pm 4.15 \times 10^5$	6.33×10^4	3.96 ± 43.03	3.96
				LNA	$3.00 \times 10^5 \pm 9.57 \times 10^5$	3.00×10^5	2.66 ± 28.32	2.66
O. dioica	11	Apr 2014 NWMS (laboratory)	0.54 ± 0.05 (0.52)	NanoEuk	$8.53 \times 10^2 \pm 0.00 \times 10^0$	8.53×10^2	**1.44 ± 0.58**	**1.12**
				PicoEuk	$6.38 \times 10^2 \pm 0.00 \times 10^0$	6.38×10^2	**2.28 ± 0.96**	**2.62**
				Syn	$4.82 \times 10^4 \pm 0.00 \times 10^0$	4.82×10^4	**1.54 ± 0.43**	**1.30**
				PLP	$1.38 \times 10^4 \pm 0.00 \times 10^0$	1.38×10^4	**1.31 ± 0.45**	**1.18**
				HNA-Ls	$1.74 \times 10^5 \pm 0.00 \times 10^0$	1.74×10^5	**0.78 ± 0.39**	**0.73**
				HNA-Hs	$2.30 \times 10^4 \pm 0.00 \times 10^0$	2.30×10^4	**0.62 ± 0.36**	**0.56**
				LNA	$4.37 \times 10^5 \pm 0.00 \times 10^0$	4.37×10^5	**1.46 ± 0.45**	**1.29**
O. dioica	10	Dec 2015 North Sea (laboratory)	0.95 ± 0 (0.95)	NanoEuk	$1.6 \times 10^2 \pm 2.93 \times 10^1$	1.59×10^2	**55.19 ± 31.23**	**58.21**
				PicoEuk	$4.27 \times 10^2 \pm 5.75 \times 10^1$	4.29×10^2	**18.52 ± 9.77**	**16.89**
				Syn	$1.66 \times 10^3 \pm 1.79 \times 10^2$	1.71×10^3	**15.43 ± 6.8**	**17.08**
				PLP	$3.77 \times 10^2 \pm 4.52 \times 10^1$	4.11×10^2	**12.1 ± 10**	**8.14**
				HNA-Ls	$1.12 \times 10^5 \pm 7.39 \times 10^3$	1.11×10^5	6.55 ± 6.76	2.12
				HNA-Hs	$6.65 \times 10^4 \pm 5.57 \times 10^3$	6.62×10^4	6.36 ± 9.1	0.00
				LNA	$5.89 \times 10^4 \pm 6.30 \times 10^3$	6.12×10^4	**6.57 ± 6.38**	**2.12**

to the controls (data not shown). The ambient concentration of non-photosynthetic bacteria cells was $6 \times 10^5 \pm 1.2 \times 10^5$ cells ml^{-1} with 20 phylotypes (clustered at 98% identity), accounting for 94% of the total 16S rRNA gene reads sequenced. The SAR11 clade and pico-cyanobacterial phylotypes accounted for 52 and 25% of the total reads, respectively (pink and green shades, respectively, in Fig. 2c), and *O. fusiformis* cleared both at low rates (Fig. 2c).

Only 2 reliable samples were obtained from *in situ* incubations of *O. longicauda.* These 2 specimens showed trends similar to those observed for *O. fusiformis*, with preferential removal of the PicoEuk (19.2 ± 50 ml $ind.^{-1}$ h^{-1}; Fig. S1a,b in the Supplement, Table 1) over both the larger NanoEuk and smaller pico-cyanobacteria (13 ± 10 and 10 ± 2.9 ml $ind.^{-1}$ h^{-1} respectively; Fig. S1a,b). The abundant non-photosynthetic bacteria groups that numerically dominated the planktonic community were removed at CRs lower (2.7 to 4 ml $ind.^{-1}$ h^{-1}) than PicoEuk or NanoEuk (Table 1, Fig. S1a,b).

3.2. Particle composition on appendicularian houses

DNA extracted and sequenced (16S rRNA) from discarded houses at the end of *in situ* incubations showed marked differences between the 3 appendic-

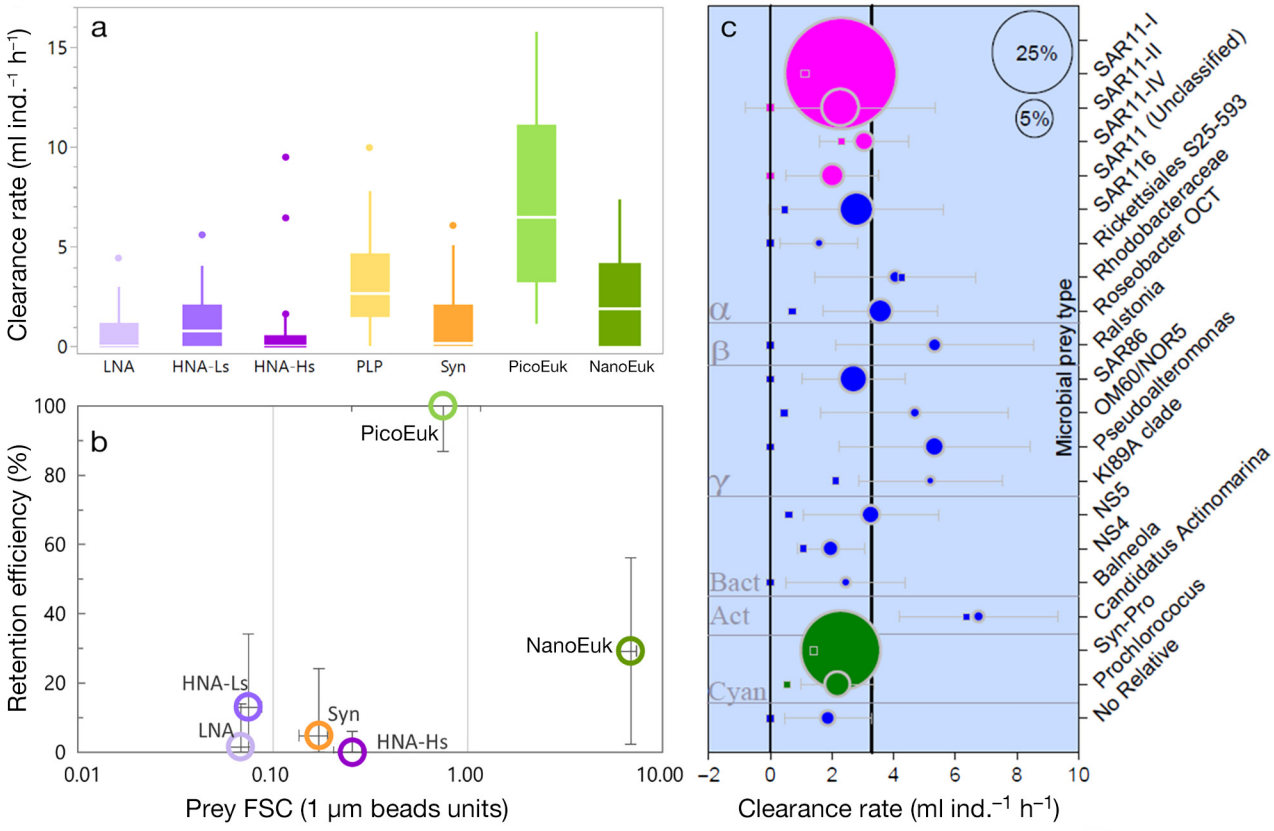

Fig. 2. Differential clearance rates of *Oikopleura fusiformis* on marine microbes, measured by *in situ* incubations in the NSMS during April 2014 (n = 22). See Fig. 1 for further details

ularian species. Due to the low sample sizes, no absolute trends can be deduced. Nevertheless, results show that the most abundant microbial phylotypes (except SAR11-II, NS4, and *Balneola*) accumulated in *O. albicans* houses (Table S1). The degree of accumulation (relative to ambient seawater) varied across phylotypes but was especially high for the K189A clade, *Pseudoalteromonas*, and *Ralstonia* (Table S1). The few houses from *O. fusiformis* and *O. longicauda* contained a very different microbial composition, with minimal change in the relative abundance of most phylotypes between the ambient water and the house. A notable exception was again the K189A clade, which was highly accumulated in the houses of all 3 species (Table S1).

3.3. Laboratory incubations

3.3.1. NWMS

Laboratory incubations of *O. dioica* at Villefranche-sur-Mer also revealed significant differential prey removal with no correlation to particle size (Fig. 3c), RM-ANOVA, Wilks' $\lambda = 0.06$, $F_{6,5} = 13.1$, $p < 0.01$). Small and abundant prey types, such as pico-cyanobacteria and LNA bacteria (Table 1), were removed at similar efficiency (Syn: 63 ± 17%; PLP: 55 ± 10%; LNA: 60 ± 17%) to the larger and much less abundant NanoEuk (55 ± 18%; Fig. 3a,c), while the intermediate-sized PicoEuk were removed at higher efficiency than all other cells (78 ± 22%; Fig. 3a,c). *O. dioica* removed bacteria from the HNA-Hs and HNA-Ls clusters, which are about the same size as Syn and LNA, respectively, with lower efficiencies (HNA-Hs: 21 ± 12%; HNA-Ls: 28 ± 11%; Fig. 3a,c).

The 16S sequencing showed that 20 phylotypes accounted for 93% of total 16S rRNA gene reads. Pico-cyanobacteria and the SAR11 clade dominated the microbial community (21 and 53%, respectively). Significant differences in removal efficiencies were found within the SAR11 clade. While *O. dioica* did not appreciably remove SAR11-I (0.3 ± 0.1 ml ind.$^{-1}$ h^{-1}; Fig. 3c), which accounted for 45% of the population, it cleared the less abundant members of that clade at significantly higher CRs (SAR11-II: 1.5 ± 0.4; SAR11-IV: 2.3 ± 0.6; and an unclassified SAR11: 2.1 ± 0.6 ml ind.$^{-1}$ h^{-1}; Fig. 3c).

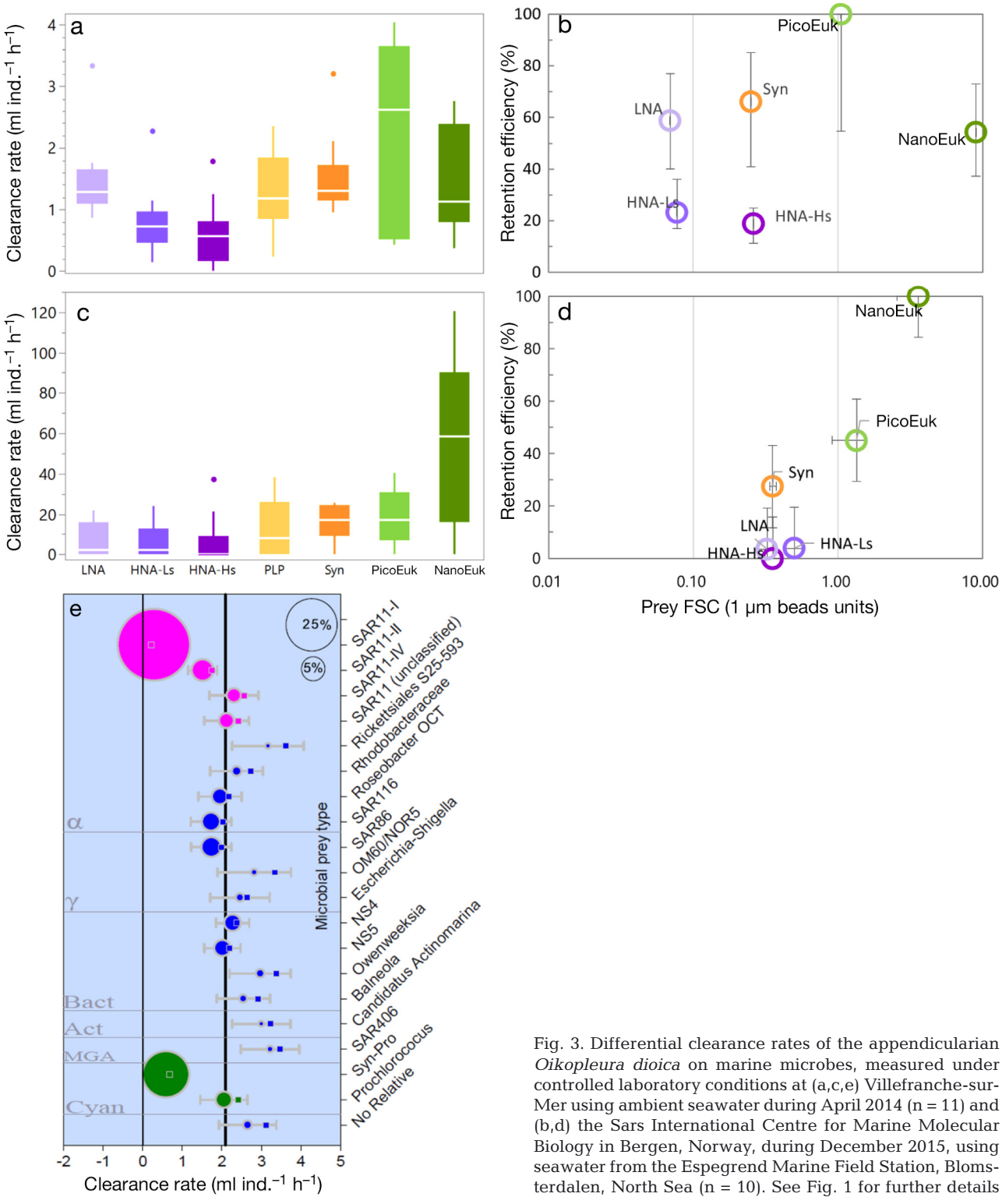

Fig. 3. Differential clearance rates of the appendicularian *Oikopleura dioica* on marine microbes, measured under controlled laboratory conditions at (a,c,e) Villefranche-sur-Mer using ambient seawater during April 2014 (n = 11) and (b,d) the Sars International Centre for Marine Molecular Biology in Bergen, Norway, during December 2015, using seawater from the Espegrend Marine Field Station, Blomsterdalen, North Sea (n = 10). See Fig. 1 for further details

3.3.2. North Sea

Ambient surface water collected in the winter from the North Sea coast of Norway (latitude: 60.2° N) contained low cell concentrations, consisting of only a few hundred eukaryotic algal cells per ml (NanoEuk: $1.1 \times 10^2 \pm 2.3 \times 10^1$; PicoEuk: $3.9 \times 10^2 \pm 2.7 \times 10^1$ cells ml^{-1}) (Fig. 3b,d, Table 1) and low concentra-

tions of non-photosynthetic bacteria ($2.3 \times 10^5 \pm 7.6 \times 10^3$ cells ml^{-1}).

Unlike our *O. dioica* incubation experiments using water from the NWMS, *O. dioica* incubated in water from the North Sea showed size-dependent selectivity, removing NanoEuk (84 ± 26%) and PicoEuk (46 ± 27%) at higher efficiencies than smaller Syn (36 ± 22%; PLP: 27 ± 27%) and non-photosynthetic bacteria (HNA-Hs: 15 ± 25%; HNA-Ls: 14 ± 17%; LNA: 13 ± 15%; Fig. 3b,d). These differences were not statistically significant, likely due to the small number of prey cells that introduced high variance in flow cytometry cell counts.

4. DISCUSSION

Appendicularians are important mesozooplankton with high individual filtration rates, but there are relatively few studies of their feeding *in situ* (Alldredge 1981, Landry et al. 1994, Acuña et al. 1999, López-Urrutia et al. 2003). These prior studies used synthetic particles (Alldredge 1981) or relied on gut pigment analysis (Landry et al. 1994, Acuña et al. 1999, López-Urrutia et al. 2003). The former technique isolates only the effect of prey size, while the latter technique has limited taxonomic resolution and misses non-pigmented microbes. Flow cytometry techniques and next-generation sequencing are relatively new tools that address some of these methodological limitations and have greatly advanced our ability to quantify feeding on microbial populations (reviewed in Sutherland & Thompson 2022). Our measurements revealed species-specific differences in appendicularian prey preferences: some species removed prey in a more size-dependent manner (*Oikopleura albicans*, *O. dioica* in the North Sea) while others did not (*O. fusiformis*, *O. longicauda*, *O. dioica* in NWMS). This is the first evaluation of the natural diet of *O. albicans*. The size ratio of appendicularians to their preferred prey (>1000:1) is higher than previous work suggests (e.g. 100:1; reviewed in Lombard et al. 2011).

It should be noted that the results provided for *O. dioica* were obtained using laboratory analysis only. Moreover, the setting of the North Sea and NWMS experiments differs to some extent (different temperatures, salinities, and incubation vessels). More importantly, the laboratory experiment with *O. dioica* in the NWMS was conducted simultaneously with the *in situ* experiments, using the same water and hence the same microbial community. In contrast, the microbial community introduced to the *O. dioica* during laboratory experiments at the North Sea was very different. These caveats hindered direct comparison between the results obtained for *O. dioica* and those for the animals that were found in the *in situ* experiments (*O. albicans*, *O. fusiformis*, *O. longicauda*).

Our results showed less efficient removal of the larger NanoEuk cells compared to PicoEuk for 3 of the 4 appendicularian species examined (*O. dioica*, *O. fusiformis*, and *O. longicauda*). This decreased retention efficiency for larger particles is similar to that observed by Fernández et al. (2004), who found small *O. dioica* exhibited decreased filtration rates for particles 3 to 6 µm. Fernández et al. (2004) suggested these results were most likely due to exclusion by the inlet filter, which limits the entrance of prey cells larger than the inlet filter mesh into the appendicularian's house. However, the appendicularians in our study were generally larger than the small *O. dioica* in Fernández et al. (2004), and it is more difficult to determine if particle size-selection by the inlet filters is the sole mechanism for our results. The pore size of the inlet filters of *O. dioica* scales linearly with the animal's body size (Lombard et al. 2010b). Therefore, pre-filter aperture size in individuals with an average body size of 0.5 mm, as used in our laboratory incubations (Table 1), is expected to be ~15 × 45 µm (Lombard et al. 2010b). This means that most of the NanoEuk (2 to 20 µm) should pass through this filter, with some caveats depending on particle shape relative to the mesh dimensions, variability of the mesh pores, and the effective mesh pore size, which may be reduced if large particles aggregate on the inlet filters.

Likewise, *O. fusiformis* removed the smallest fraction of the NanoEuk (5 to 7 µm) with lower efficiency than PicoEuk. Although the dimensions of the filter apertures in *O. fusiformis* are unknown, its larger body size (average 0.67 mm in the specimens we used) suggests the mesh pores of the pharyngeal filter are likely larger than those of *O. dioica* (Deibel & Powell 1987). Since patterns of cell removal in *O. longicauda* and *O. fusiformis* were similar and since *O. longicauda* has no inlet filters, we suggest that *O. longicauda* does not use size-dependent mechanical filtration for larger cells.

A different pattern was observed for *O. albicans*, the largest species (1.99 mm) we worked with, which generally removed particles in correlation with size. However, within the submicron-size class of particles, *O. albicans* retained submicron bacteria with different efficiencies depending on phylotypes (Fig. 1). In particular, members of the SAR11 clade, SAR116,

and *Pseudoalteromonas* were retained at significantly lower efficiency, whereas pico-cyanobacteria were 'preferentially' removed. Since it is unlikely that these differences are related to the cell sizes, this suggests other mechanisms such as cell surface properties are involved in the observed differential retention efficiencies for submicron particles (Dadon-Pilosof et al. 2017).

CRs are a common measure of suspension-feeding rates that are essentially a product of the organism's water processing (pumping) rate and filtration efficiency. In the appendicularian literature, CRs are represented in one of 2 ways: (1) as a single value representing the volume of water cleared of planktonic cells per unit time (e.g. Tiselius et al. 2003), often used synonymously with pumping rates; or (2) as multiple values, each specific to a particular prey population (Sommer et al. 2002, Fernández et al. 2004, Tönnesson et al. 2005). Our findings of differential retention suggest that appendicularian CRs cannot be calculated as a single number; instead, prey-specific rates should be used.

In our analysis, the prey population is defined either by the cytometric divisions based on prey size, fluorescence, and cell content or by the sequencing analysis down to the OTU level (phylotype level). Using this analysis, we suggest that the maximal prey-specific CRs recorded per appendicularian species should be used as the best estimate of the water processing (pumping) rate. Our results showed that for *O. fusiformis*, *O. longicauda*, and *O. dioica*, PicoEuk cells were removed at the highest CRs (7.4 ± 2.1, 19.2 ± 50.3, and 2.3 ± 1.0 ml ind.$^{-1}$ h^{-1}, respectively), which are similar to or higher than previously reported values (Deibel 1997, Sato et al. 2004).

CR quantifies which prey the appendicularians removed from the water and at what rate, but not all removed prey are necessarily ingested. Some of the prey populations may be retained in the house (Gorsky et al. 1984, Bochdansky & Deibel 1999, Fernández et al. 2004, Conley & Sutherland 2017, Conley et al. 2018a). This results in at least 4 different potential fates for the retained prey populations: (1) prey cells that are ingested by the animal will contribute to appendicularian biomass and metabolism and the by-product of fecal pellets (Fig. 4); (2) concentrated microbes attached to the appendicularian house can be eaten by larger zooplankton and small fish that would not otherwise be able to filter small particles directly from the water (Alldredge 1976b); (3) cells that are retained in the house but have not been ingested will sink with it when it is discarded (Table S1) and contribute to differential export of planktonic carbon to depth as marine snow (Alldredge & Silver 1988); and (4) some cells will be released from the disintegrating house back to the water column as a plume of particles (Lombard & Kiørboe 2010) and may return to the active microbial community, potentially enriched with nutrients excreted by the appendicularians (Lundgreen et al. 2019). This differentiation emphasizes the importance of using prey-specific CRs and also analyzing the microbial composition of freshly discarded houses (Table S1). By defining CR in relation to prey type, together with the composition of what is not actually ingested but retained within discarded houses, we can better quantify the contribution of specific prey to appendicularian physiology and to biogeochemical cycles in the oceans.

When considering the contribution of different prey types to the diet and growth processes of appendicularians, the biomass and abundance of each prey type in the ambient water should be considered. We calculated the contribution of each prey type to the appendicularian diet as the product of its CR, measured concentrations, and the carbon content per cell estimated using conversion factors from Houlbrèque et al. (2006) and Buitenhuis et al. (2012), as detailed in Table 2. Although non-photosynthetic bacteria were removed at lower rates than all other prey groups (Figs. 1 to 3), due to their high abundance, their total contribution to the appendicularian diet was not trivial: it represented 5 to 19% of the planktonic carbon in the appendicularian diet. This contribution was similar to, and sometimes even higher than, the contribution of the much 'preferred' but less-abundant PicoEuk (Tables 1 & 2) that appendicularians cleared at the highest efficiency. Due to their large biovolume, NanoEuk accounted for most of the planktonic carbon removed by the appendicularians (40 to 70% of the total), despite generally lower numerical abundances (Table 2). The relative removal of prey types and their contributions to diet are thus driven by both differential capturability and available background prey. During blooms, appendicularians can remove more than half of the marine microbial populations in a matter of days (Alldredge 1981, Scheinberg et al. 2005), thus playing a central role in pelagic food webs (D'Alelio et al. 2016). Information on prey preferences provides us with the capacity to predict removal rates for different ambient prey assemblages.

Appendicularians can exhibit considerably lower prey-to-predator ratios than most planktonic groups (compare Lombard et al. 2011 to Boyce et al. 2015), and thus they shorten the food chain by directly

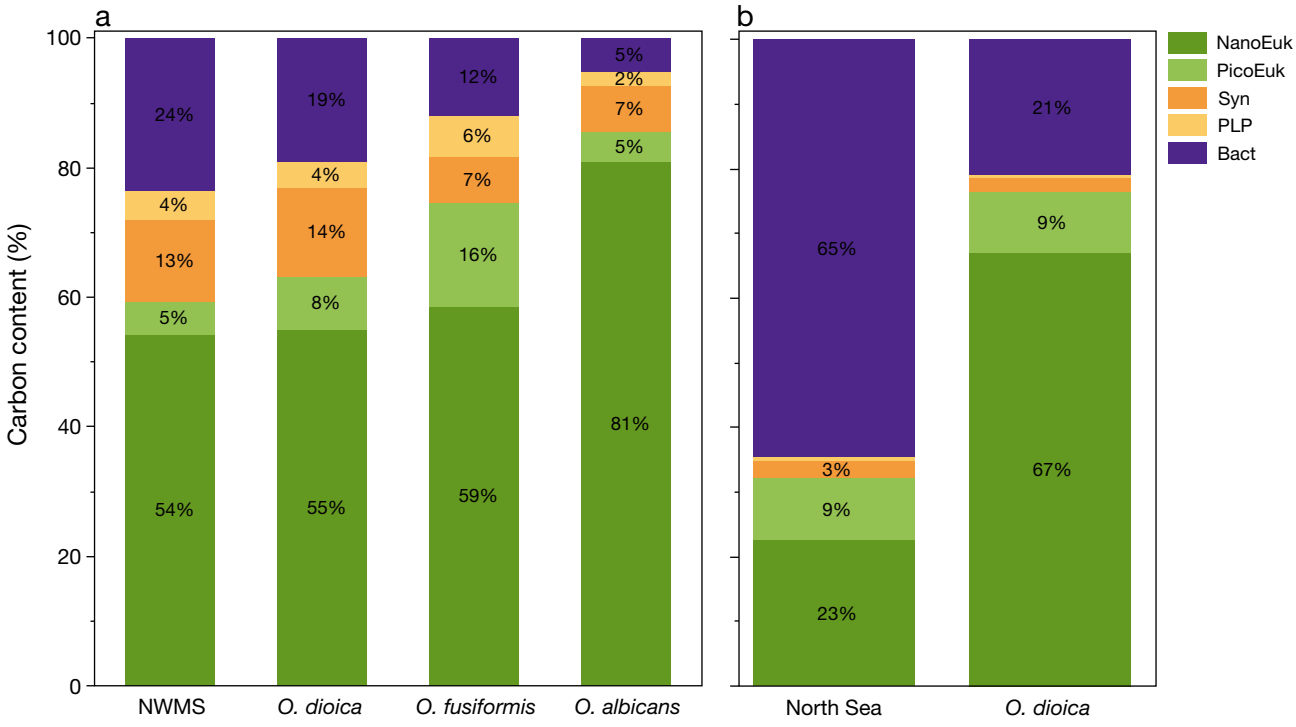

Fig. 4. Relative contribution (%) of the dominant microbial populations to planktonic carbon in the ambient water during sampling and to appendicularians' diet based on clearance rates for (a) *Oikopleura albicans* (n = 16), *O. dioica* (n = 11), and *O. fusiformis* (n = 22) in the Northwest Mediterranean Sea (NWMS) and (b) *O. dioica* (n = 10) and the sampling site in the North Sea. Calculations are based on measured concentrations of each prey population and estimated carbon content per cell for each population from Houlbrèque et al. (2006) and Buitenhuis et al. (2012), as detailed in Table 2. All abbreviations are as in Fig. 1

Table 2. Estimated contribution of dominant microbial populations to planktonic biomass in appendicularian diets as sampled in the Northwest Mediterranean Sea for *Oikopleura albicans*, *O. dioica*, and *O. fusiformis* and in the North Sea for *O. dioica*. Calculations are based on the measured concentration of each prey population and published conversion factors. This is a summary table; detailed statistics for each parameter are reported in Table 1 and group acronyms are defined in Fig. 1. Amb. conc.: average ambient concentration; CC: conversion factor–carbon content per cell

Group			Northwest Mediterranean Sea						North Sea *O. dioica*		
			Average clearance rate (l ind.$^{-1}$ h^{-1})			Carbon content in diet (µg ind.$^{-1}$ h^{-1})					
	CC (fg C cell^{-1})	Amb. conc. (cells ml^{-1})	*O. albicans*	*O. dioica*	*O. fusiformis*	*O. albicans*	*O. dioica*	*O. fusiformis*	Amb. conc. (cells ml^{-1})	Clearance rate (l ind.$^{-1}$ h^{-1})	Carbon content in diet (µg ind.$^{-1}$ h^{-1})
NanoEuk[a]	7628	1.7×10^3	0.024	0.001	0.003	0.319	0.019	0.034	1.1×10^2	0.055	0.046
PicoEuk[b]	1319	1.4×10^3	0.014	0.002	0.007	0.027	0.004	0.014	3.9×10^2	0.019	0.010
Syn[b]	154	5.0×10^4	0.009	0.002	0.001	0.070	0.012	0.010	1.6×10^3	0.015	0.004
PLP[b]	60	1.9×10^4	0.008	0.001	0.003	0.009	0.002	0.004	3.8×10^2	0.012	0.000
Bact[a]	14	5.7×10^5	0.004	0.001	0.001	0.028	0.009	0.010	2.3×10^5	0.006	0.020

[a]Houlbrèque et al. (2006); [b]Buitenhuis et al. (2012)

transferring pico-planktonic biomass and energy to higher levels of the food web (Gorsky & Fenaux 1998). This ratio becomes even more important in oligotrophic systems, where pico-planktonic cells dominate the planktonic communities (Gorsky & Fenaux 1998). Our findings revealed prey–predator size ratios similar to those cited by Boyce et al. (2015) only when assuming that the large NanoEuk are the main prey type of the appendicularians (Fig. 5, black downward-facing triangles). Previous studies may have indiscriminately averaged all prey types together, and the much larger

NanoEuk would clearly dominate such calculations. Our strategy of calculating a separate CR for each prey type reveals much lower prey-to-predator size ratios, ranging between ~1:1000 and 1:2000 (Table 2, Fig. 5), as was also reported by Gorsky & Fenaux (1998). The removal of micron and submicron prey at high rates underscores the influence that appendicularians have on the microbial loop (Gorsky et al. 1999, Calbet & Landry 2004).

Appendicularians have one of the most complex filtration processes in the animal kingdom. In addition to the physical complexity of the filter, our results indicate that there is also complexity in terms of how this filter interacts with biological particles—revealing some intriguing selectivity patterns that do not depend solely on particle size. The impact of appendicularians on marine microbial assemblages, especially during their blooms, depends on the structure of the inlet, food-concentrating, and pharyngeal filters and also on the degree to which particles are concentrated, attached, or may slip through those different layers of mesh. Appendicularians can also actively reject prey based on the chemical characteristics of the particles (Lombard et al. 2011). Collectively, our results show how these processes may manifest in the natural diet of these species at the prey phylotype level. Prey-specific filtration should be considered in future models of marine food webs.

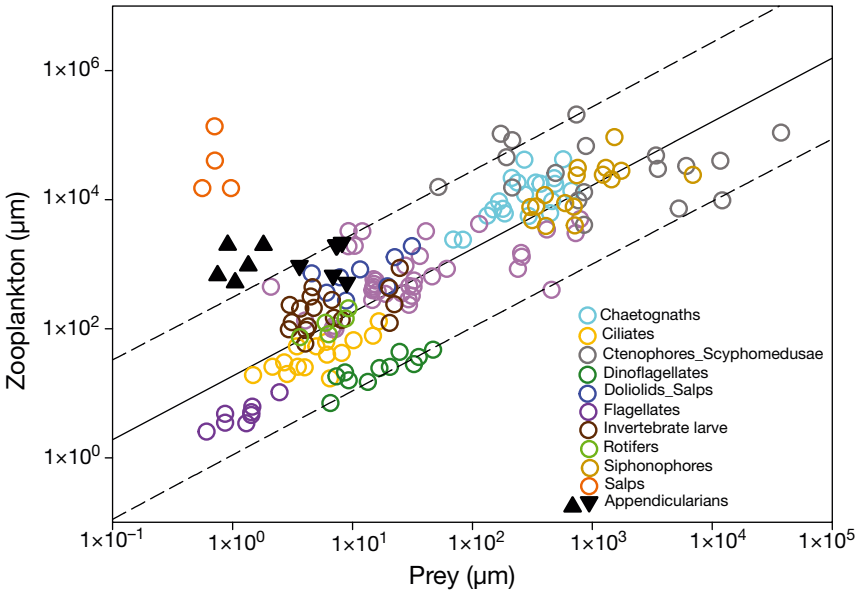

Fig. 5. Size-based relationships between appendicularians and their prey from *in situ* and laboratory measurements (this study, black triangles) plotted along with predictions and observations for size-based predation in planktonic food webs obtained from the literature (circles). Upward-pointing triangles: appendicularians feeding on PicoEuk; downward-pointing triangles: appendicularians feeding on NanoEuk. Dark orange circles: measurements of salps feeding on their main food source (PicoEuk), derived from *in situ* experiments (Dadon-Pilosof et al. 2019). Other planktonic predators represented by circles were adapted (with permission) from Boyce et al. (2015). Solid line: linear regression fit; dashed lines: 95% predictions interval (for Boyce et al. 2015 data)

Acknowledgements. Research funding was provided by BSF grant 2012089 to K.R.S. and G.Y.; BSF grant 2017622 to G.Y.; ISF grant 1280/13 and 249/21 to G.Y.; ECOGELY ANR-10-PDOC-005-01 to F.L.; NSF 1537201 to K.R.S.; and support provided to A.D.P by the Mediterranean Sea Research Center of Israel (MRCI). This work was supported by EMBRC-France, whose French state funds are managed by the ANR within the Investments of the Future program under reference ANR-10-INBS-02. We thank M. Gilboa and R. Rosenblatt for technical and diving assistance and Jean-Marie Bouquet for assistance with the setup of experiments and care of cultured animals, Eric Thompson for use of the Sars Center resources, and the staff at Appendic Park for assistance maintaining cultured animals.

LITERATURE CITED

Acuña JL, Deibel D, Morris CC (1996) Particle capture mechanism of the pelagic tunicate *Oikopleura vanhoeffeni*. Limnol Oceanogr 41:1800–1814

Acuña JL, Deibel D, Bochdansky AB, Hatfield E (1999) *In situ* ingestion rates of appendicularian tunicates in the Northeast Water Polynya (NE Greenland). Mar Ecol Prog Ser 186:149–160

Alldredge AL (1976a) Appendicularians. Sci Am 235: 94–105

Alldredge AL (1976b) Discarded appendicularian houses as sources of food, surface habitats, and particulate organic matter in planktonic environments. Limnol Oceanogr 21: 14–23

Alldredge AL (1976c) Field behavior and adaptive strategies of appendicularians (Chordata: Tunicata). Mar Biol 38: 29–39

Alldredge AL (1977) House morphology and mechanisms of feeding in the Oikopleuridae (Tunicata, Appendicularia). J Zool 181:175–188

Alldredge AL (1981) The impact of appendicularian grazing on natural food concentrations *in situ*. Limnol Oceanogr 26:247–257

Alldredge AL, Silver MW (1988) Characteristics, dynamics and significance of marine snow. Prog Oceanogr 20:41–82

Bedo AW, Acuña JL, Robins D, Harris R (1993) Grazing in the micron and the sub-micron particle size range: the case of *Oikopleura dioica* (Appendicularia). Bull Mar Sci 53:2–14

Bochdansky AB, Deibel D (1999) Functional feeding response and behavioral ecology of *Oikopleura vanhoeffeni* (Appendicularia, Tunicata). J Exp Mar Biol Ecol 233:181–211

Boyce DG, Frank KT, Leggett WC (2015) From mice to elephants: overturning the 'one size fits all' paradigm in marine plankton food chains. Ecol Lett 18:504–515

Brown MV, Lauro FM, DeMaere MZ, Muir L and others (2012) Global biogeography of SAR11 marine bacteria. Mol Syst Biol 8:595

Buitenhuis E, Li W, Vaulot D, Lomas MW and others (2012) Picophytoplankton biomass distribution in the global ocean. Earth Syst Sci Data 4:37–46

Calbet A, Landry MR (2004) Phytoplankton growth, microzooplankton grazing, and carbon cycling in marine systems. Limnol Oceanogr 49:51–57

Camacho C, Coulouris G, Avagyan V, Ma N, Papadopoulos J, Bealer K, Madden TL (2009) BLAST+: architecture and applications. BMC Bioinformatics 10:1–9

Carlson CA, Morris R, Parsons R, Treusch AH, Giovannoni SJ, Vergin K (2009) Seasonal dynamics of SAR11 populations in the euphotic and mesopelagic zones of the northwestern Sargasso Sea. ISME J 3:283–295

Chesson J (1978) Measuring preference in selective predation. Ecology 59:211–215

Chesson J (1983) The estimation and analysis of preference and its relationship to foraging models. Ecology 64: 1297–1304

Conley KR, Sutherland KR (2017) Particle shape impacts export and fate in the ocean through interactions with the globally abundant appendicularian *Oikopleura dioica*. PLOS ONE 12:e0183105

Conley KR, Gemmell BJ, Bouquet J, Thompson EM, Sutherland KR (2018a) A self-cleaning biological filter: how appendicularians mechanically control particle adhesion and removal. Limnol Oceanogr 63:927–938

Conley KR, Lombard F, Sutherland KR (2018b) Mammoth grazers on the ocean's minuteness: a review of selective feeding using mucous meshes. Proc R Soc B 285:20180056

Cunningham A, Buonnacorsi GA (1992) Narrow-angle forward light scattering from individual algal cells: implications for size and shape discrimination in flow cytometry. J Plankton Res 14:223–234

D'Alelio D, Libralato S, Wyatt T, Ribera d'Alcalà M (2016) Ecological-network models link diversity, structure and function in the plankton food-web. Sci Rep 6:1806

Dadon-Pilosof A, Conley KR, Jacobi Y, Haber M and others (2017) Surface properties of SAR11 bacteria facilitate grazing avoidance. Nat Microbiol 2:1608–1615

Dadon-Pilosof A, Lombard F, Genin A, Sutherland KR, Yahel G (2019) Prey taxonomy rather than size determines salp diets. Limnol Oceanogr 64:1996–2010

Dagg MJ, Green EP, McKee BA, Ortner PB (1996) Biological removal of fine-grained lithogenic from a large river plume particles. J Mar Res 54:149–160

Davis CS (2002) Statistical methods for the analysis of repeated measurements. Springer, New York, NY

Deibel D (1985) Clearance rates of the salp *Thalia democratica* fed naturally occurring particles. Mar Biol 86:47–54

Deibel D (1997) Feeding and metabolism of appendicularians. In: Bone Q (ed) The biology of pelagic tunicates. Oxford University Press, Oxford, p 139–149

Deibel D, Lee SH (1992) Retention efficiency of sub-micrometer particles by the pharyngeal filter of the pelagic tunicate *Oikopleura vanhoeffeni*. Mar Ecol Prog Ser 81:25–30

Deibel D, Powell CVL (1987) Comparison of the ultrastructure of the food-concentrating filter of two appendicularians. Mar Ecol Prog Ser 39:81–85

Fernández D, López-Urrutia Á, Fernández A, Acuña JL, Harris R (2004) Retention efficiency of 0.2 to 6 µm particles by the appendicularians *Oikopleura dioica* and *Fritillaria borealis*. Mar Ecol Prog Ser 266:89–101. Corrigendum (2015) 533:291

Flood PR, Deibel D, Morris CC (1992) Filtration of colloidal melanin from sea water by planktonic tunicates. Nature 355:630–632

Garcia NS, Bonachela JA, Martiny AC (2016) Interactions between growth-dependent changes in cell size, nutrient supply and cellular elemental stoichiometry of marine *Synechococcus*. ISME J 10:2715–2724

Gerritsen J, Porter KG (1982) The role of surface chemistry in filter feeding by zooplankton. Science 216:1225–1227

Gorsky G, Fenaux R (1998) The role of appendicularians in marine food webs. In: Bone Q (ed) The biology of pelagic tunicates. Oxford University Press, Oxford, p 161–169

Gorsky G, Fisher NS, Fowler SW (1984) Biogenic debris from the pelagic tunicate, *Oikopleura dioica*, and its role in the vertical transport of a transuranium element. Estuar Coast Shelf Sci 18:13–23

Gorsky G, Chrétiennot-Dinet MJ, Blanchot J, Palazzoli I (1999) Picoplankton and nanoplankton aggregation by appendicularians: fecal pellet contents of *Megalocercus huxleyi* in the equatorial Pacific. J Geophys Res 104: 3381–3390

Harbison GR, McAlister VL (1979) The filter-feeding rates and particle retention efficiencies of three species of *Cyclosalpa* (Tunicata, Thaliacea). Limnol Oceanogr 24: 875–892

Hopcroft RR, Robison BH (1999) A new mesopelagic larvacean, *Mesochordaeus erythrocephalus*, sp. nov., from Monterey Bay, with a description of its filtering house. J Plankton Res 21:1923–1937

Hopcroft RR, Roff JC (1998) Production of tropical larvaceans in Kingston Harbour, Jamaica: Are we ignoring an important secondary producer? J Plankton Res 20:557–569

Houlbrèque F, Delesalle B, Blanchot J, Montel Y, Ferrier-Pagès C (2006) Picoplankton removal by the coral reef community of La Prévoyante, Mayotte Island. Aquat Microb Ecol 44:59–70

Jacobi Y, Shenkar N, Ward JE, Rosa M, Ramon GZ, Shavit U, Yahel G (2021) Evasive plankton: size-independent particle capture by ascidians. Limnol Oceanogr 66: 1009–1020

King KRI, Hoilibaugh JT, Azam F (1980) Predator–prey interactions between the larvacean *Oikopleura dioica* and bacterioplankton in enclosed water columns. Mar Biol 56: 49–57

Landry MR, Peterson WK, Fagerness VL (1994) Mesozooplankton grazing in the Southern California Bight. I. Population abundances and gut pigment contents. Mar Ecol Prog Ser 115:55–71

Lawrence J, Joachim T, Bratbak G, Larsen A, Thompson E, Troedsson C, Ray JL (2018) Viruses on the menu: the appendicularian *Oikopleura dioica* efficiently removes viruses from seawater. Limnol Oceanogr 63:S244–S253

Li W, Godzik A (2006) Cd-hit: a fast program for clustering and comparing large sets of protein or nucleotide sequences. Bioinformatics 22:1658–1659

Lombard F, Kiørboe T (2010) Marine snow originating from appendicularian houses: age-dependent settling characteristics. Deep Sea Res I 57:1304–1313

Lombard F, Legendre L, Picheral M, Sciandra A, Gorsky G (2010a) Prediction of ecological niches and carbon export by appendicularians using a new multispecies ecophysiological model. Mar Ecol Prog Ser 398:109–125

Lombard F, Eloire D, Gobet A, Stemmann L, Dolan JR, Sciandra A, Gorsky G (2010b) Experimental and modeling evidence of appendicularian–ciliate interactions. Limnol Oceanogr 55:77–90

Lombard F, Selander E, Kiørboe T (2011) Active prey rejection in the filter-feeding appendicularian *Oikopleura dioica*. Limnol Oceanogr 56:1504–1512

López-Urrutia Á, Acuña JL, Irigoien X, Harris R (2003) Food limitation and growth in temperate epipelagic appendicularians (Tunicata). Mar Ecol Prog Ser 252:143–157

Lundgreen RBC, Jaspers C, Traving SJ, Ayala DJ and others (2019) Eukaryotic and cyanobacterial communities associated with marine snow particles in the oligotrophic Sargasso Sea. Sci Rep 9:8891

Marie D, Brussaard CPD, Thyrhaug R, Bratbak G and others (1999) Enumeration of marine viruses in culture and natural samples by flow cytometry. Appl Environ Microbiol 65: 45–52

Mary I, Heywood JL, Fuchs BM, Amann R, Tarran GA, Burkill PH, Zubkov MV (2006) SAR11 dominance among metabolically active low nucleic acid bacterioplankton in surface waters along an Atlantic meridional transect. Aquat Microb Ecol 45:107–113

Morris RM, Vergin KL, Cho JC, Rappé MS, Carlson CA, Giovannoni SJ (2005) Temporal and spatial response of bacterioplankton lineages to annual convective overturn at the Bermuda Atlantic Time-series Study site. Limnol Oceanogr 50:1687–1696

Partensky F, Hess WR, Vaulot D (1999) *Prochlorococcus*, a marine photosynthetic prokaryote of global significance. Microbiol Mol Biol Rev 63:106–127

Pruesse E, Peplies J, Glöckner FO (2012) SINA: accurate high-throughput multiple sequence alignment of ribosomal RNA genes. Bioinformatics 28:1823–1829

Quast C, Pruesse E, Yilmaz P, Gerken J and others (2013) The SILVA ribosomal RNA gene database project: improved data processing and web-based tools. Nucleic Acids Res 41:D590–D596

Riisgård HU (2001) On measurement of filtration rate in bivalves—the stony road to reliable data: review and interpretation. Mar Ecol Prog Ser 211:275–291

Robertson BR, Button DK (1989) Characterizing aquatic bacteria according to population, cell size, and apparent DNA content by flow cytometry. Cytometry 10:70–76

Rubenstein DI, Koehl MAR (1977) The mechanisms of filter feeding: some theoretical considerations. Am Nat 111: 981–994

Sato R, Tanaka Y, Ishimaru T (2004) Clearance and ingestion rates of three appendicularian species, *Oikopleura longicauda*, *O. rufescens* and *O. fusiformis*. In: Gorsky G, Youngbluth MJ, Deibel D (eds) Response of marine ecosystems to global change: ecological impact of appendicularians. Éditions Scientifiques GB, Paris, p 197–212

Scheinberg RD, Landry MR, Calbet A (2005) Grazing of two common appendicularians on the natural prey assemblage of a tropical coastal ecosystem. Mar Ecol Prog Ser 294:201–212

Selander E, Tiselius P (2003) Effects of food concentration on the behaviour of *Oikopleura dioica*. Mar Biol 142:263–270

Silvester NRR (1983) Some hydrodynamic aspects of fitter feeding with rectangular-mesh nets. J Theor Biol 103: 265–286

Simon N, Barlow GR, Marie D, Partensky F, Vaulot D (1994) Characterization of oceanic photosynthetic picoeukaryotes by flow cytometery. J Phycol 30:922–935

Sommer U, Berninger UG, Böttger-Schnack R, Cornils A and others (2002) Grazing during early spring in the Gulf of Aqaba and the Northern Red Sea. Mar Ecol Prog Ser 239: 251–261

Sutherland KR, Thompson AW (2022) Pelagic tunicate grazing on marine microbes revealed by integrative approaches. Limnol Oceanogr 67:102–121

Suzuki MT, Béjà O, Taylor LT, Delong EF (2001) Phylogenetic analysis of ribosomal RNA operons from uncultivated coastal marine bacterioplankton. Environ Microbiol 3: 323–331

Tarao M, Jezbera J, Hahn MW (2009) Involvement of cell surface structures in size-independent grazing resistance of freshwater *Actinobacteria*. Appl Environ Microbiol 75: 4720–4726

Tiselius P, Petersen JK, Nielsen TG, Maar M and others (2003) Functional response of *Oikopleura dioica* to house clogging due to exposure to algae of different sizes. Mar Biol 142:253–261

Tönnesson K, Maar M, Vargas C, Møller EF and others (2005) Grazing impact of *Oikopleura dioica* and copepods on an autumn plankton community. Mar Biol Res 1: 365–373

Uysal Z (2001) Chroococcoid cyanobacteria *Synechococcus* spp. in the Black Sea: pigments, size, distribution, growth and diurnal variability. J Plankton Res 23:175–190

Vergin KL, Beszteri B, Monier A, Thrash JC and others (2013) High-resolution SAR11 ecotype dynamics at the Bermuda Atlantic Time-series Study site by phylogenetic placement of pyrosequences. ISME J 7:1322–1332

Worden AZ, Not F (2008) Ecology and diversity of picoeukaryotes. In: Kirchman DL (ed) Microbial ecology of the oceans. Wiley-Blackwell, Hoboken, NJ, p 159–205

Zubkov MV, Allen JI, Fuchs BM (2004) Coexistence of dominant groups in marine bacterioplankton community: a combination of experimental and modelling approaches. J Mar Biol Assoc UK 84:519–529

Editorial responsibility: Stephen Wing, Dunedin, New Zealand
Reviewed by: J. L. Acuña and 1 anonymous referee, and previous version reviewed in MEPS by 3 anonymous referees

Submitted: August 31, 2022
Accepted: December 15, 2022
Proofs received from author(s): February 17, 2023